The Influence of Coastal Morphology on the Wave Climate and Wave Energy Resource of the West Irish Coast

Roxana Tiron
School of Mathematical Sciences
UCD Dublin, Ireland
E-mail:roxana.tiron@ucd.ie

Sarah Gallagher
School of Mathematical Sciences
UCD Dublin, Ireland
E-mail: sarah.gallagher.3@ucdconnect.ie

Frédéric Dias
School of Mathematical Sciences
UCD Dublin, Ireland
E-mail: frederic.dias@ucd.ie

***Abstract*—The wave climate and wave resource for two sites on the western coast of Ireland which possess steep bathymetric gradients and complex shorelines are investigated. One is situated in the southern part of Achill Island on the Co. Mayo coastline, whereas the second is centered at Killard point on the Co. Clare coast. The wave climate is estimated using the third generation spectral wave model WAVEWATCH III, forced with directional wave spectral data and 10m winds obtained from the European Centre for Medium Range Weather Forecast (ECMWF) archive. The local area models are validated with wave buoy and Acoustic Doppler Current Profiler (ADCP) data for intermediate to shallow depths (50m or less) obtained from the ESB's WestWave project. Our results show that for an accurate representation of the directionality in the nearshore, in particular for steep bathymetric slopes found at the cliffs and exposed rocky shores of the Irish coastline, reflection needs to be accounted for. It has been found that reflection affects mainly the directional spread of the resource and to a lesser degree the significant wave height.**

***Index Terms*—wave climate, wave energy, nearshore**

I. Introduction

Wave climate studies for the western coast of Ireland have focused predominantly on the offshore [1]–[4]. At the same time, we are witnessing a paradigm shift within the operational wave forecasting community, with greater attention being payed to the nearshore. This shift was spurred in part by the increase in coastal hazards in recent decades, but also by the renewed interest in harnessing the energy of the ocean. Indeed, recent studies have shown that nearshore locations can attain wave energy levels nearly as high as in the offshore [5]. Furthermore, the adjacency to the coast will likely reduce the cost of power transport onshore and will facilitate access for maintenance.

The Irish coast presents a complicated geomorphology which will likely induce a significant variation in the wave energy resource. With this in mind, we investigate the wave climate and wave resource for two sites on the western coast of Ireland which possess steep bathymetry gradients and complex shorelines – see Figure 1. One is situated in the southern part of Achill Island on the Co. Mayo coastline whereas the second is centered at Killard point on the Co. Clare coast.

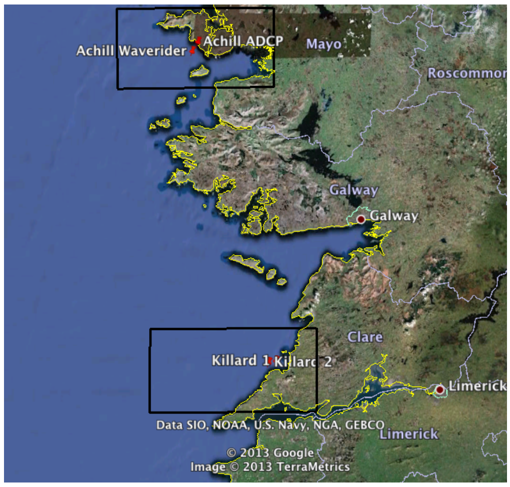

Fig. 1. Achill Island area, Co. Mayo (upper panel) and Killard Point, Co. Clare (lower panel). Wave buoys used for validation are shown with red markers.

The wave climate is estimated using the third generation spectral wave model WAVEWATCH III [6], forced with directional wave spectral data and 10m winds obtained from the European Centre for Medium-Range Weather Forecasts (ECMWF) archive. The local area models are validated with wave buoy and Acoustic Doppler Current Profiler (ADCP) data for intermediate to shallow depths (50m or less) obtained from the ESBs WestWave project [7]. Particular emphasis has been placed on coastal reflection, which has only recently been implemented in spectral wave models [8]. In our simulations we have used the parametrization for source terms and dissipation formulated in [9]. Our results show that for an accurate representation of the directionality in the nearshore, in particular for steep bathymetric slopes found at the cliffs and exposed rocky shores of the Irish coastline, reflection needs to be accounted for. It has been found that reflection affects mainly the directional spread of the resource and to a lesser degree the significant wave height. Another focus of this study is directionality, which plays a key role in the site selection, design and performance of nearshore Wave Energy

Converters (WECs). Our results show a clear variability in the wave energy resource both along the coastline and along depth gradients. Additionally, this study identifies a significant extent of the coastline which exhibits a rapid transition between the 50m depth contour and the shoreline. For these regions the energy levels are not significantly dissipated by bottom friction and thus such places might be particularly suitable as wave energy sites.

The paper is organized as follows. In §II we perform a validation check for the wind forcing and boundary input by comparison with in-situ measurements from the Irish Buoy Network. In §III we present details on the set-up of the two area models and on the construction of the bathymetric grids. In §IV we discuss our results whereas in §V we summarize our conclusions.

II. Boundary input and wind forcing quality assessment

Ocean wave forecasting is by now a well established science with many existing global and regional operational wave models at meteorological centres around the world (for example WAM at the European Centre for Medium-Range Weather Forecast ECMWF [10] or WAVEWATCH at U.S. National Oceanic and Atmospheric Administration NOAA [6]) having greatly improved accuracy in the offshore [11], especially with the assimilation of altimeter and SAR satellite data. However, it is clear that these global wave models can have limitations to how fine their spatial resolution can be reduced, due to the vast computational cost. This can cause coastal areas, especially shorelines with a complex geomorphology, to be insufficiently resolved, particularly in intermediate and shallow depths ($\leq$ 40-50m). Towards the shoreline, the resolution of a wave model may need to be in the order of tens of metres as processes have strong non-linearities and phase-averaged models can have limitations. In order to examine the nearshore wave climate for the selected locations of interest on the west coast of Ireland, several local area models (LAMs) with a very high spatial resolution were constructed using WAVEWATCH III [6]. The LAM hindcasts were then driven at the boundary by high quality wave directional spectra and over the entire domain by 10m winds (henceforth U_{10}) from the European Centre for Medium-Range Weather Forecast (ECMWF) operational archive, MARS.

Contained in the ECMWF MARS archive are operational (forecast and analysis) meteorological data and also long-term reanalysis datasets such as ERA-INTERIM. The ECMWF Integrated Forecasting System IFS3 contains an atmospheric model, an ocean wave model and an ocean circulation model. Currently the WAM model has been coupled to the operational atmospheric forecast model [12]. A coupled ocean, wave and atmospheric model is planned at the ECMWF in the near future.

Meteorological wind and wave data from the operational analysis archive, which has a higher spatial resolution then the reanalysis dataset, was used to drive the LAMs. U_{10} winds from the atmospheric model currently have a spatial

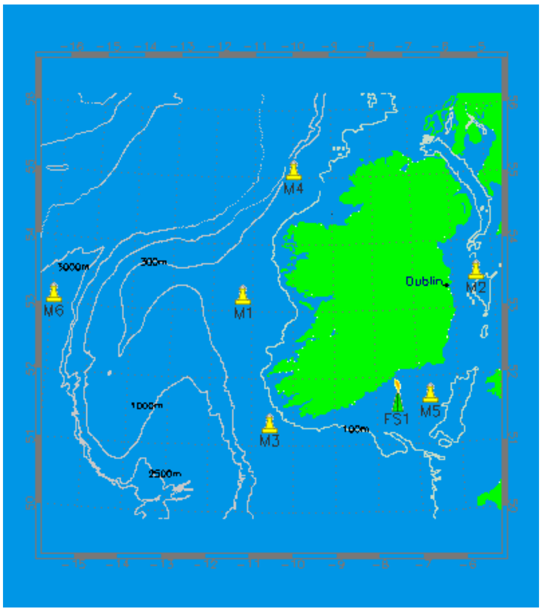

Fig. 2. Irish Marine Weather Buoy Network. Retrieved from [13].

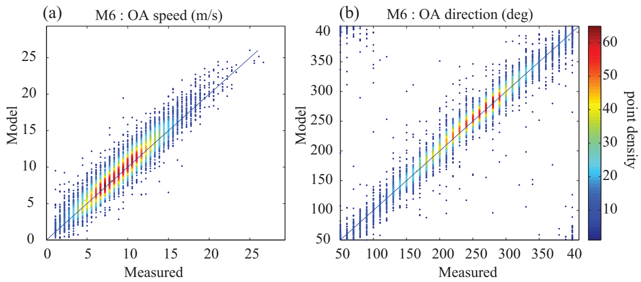

Fig. 3. Scatter diagrams for wind speed (a) and direction (b) for the M6 buoy versus OA ECMWF from 2006-2011.

resolution of about 16km on a reduced Gaussian grid and temporal resolution of the four standard synoptic times (0, 6, 12, 18 UTC) [14]. Directional wave spectra from the ECMWF European wave model analysis has a spectral resolution of 36 frequencies and 36 directions with the same temporal resolution of the four standard synoptic times.

As the ECMWF WAM operational analysis data does not assimilate buoy data [15], [16], a quality check was carried out between this and the wave data measured by the M4 deep water buoy from the Irish Marine Weather Buoy Network located at 10 °W, 55 °N, to the north-west coast of Ireland as seen in Figure 2. This validation check carried out by [17] indicates that the ECMWF WAM Operational Archive (OA) spectral wave data (from the wave model analysis) is a reliable boundary forcing source for nearshore high-resolution wave models.

In order to assess the quality of the U_{10} input, a quality check of the ECMWF OA atmospheric model analysis U_{10}, and a comparison to the ERA-INTERIM (EI) Reanalysis dataset U_{10} was performed through comparison with wind data observations at the M1, M3, M4 and M6 buoys from the

Irish Marine Weather Buoy Network installed and maintained by the Marine Institute, Met Éireann and the UK Met Office [13]. These wind measurements are taken from an anemometer at the top of the buoy at a height of 4.5m [18]. These were adjusted to 10m using the simple logarithmic conversion with height for wind in the atmospheric boundary layer found in [19]. The validation check was carried out over all periods where buoy data was available from 2001 onwards. ECMWF OA analysis and EI U_{10} data was linearly interpolated to each of the different buoy locations. The root mean square error (RMSE), bias, Pearson correlation coefficient (r) and scatter index (SI) were compared for both wind speed and direction as can be seen in Table I. Directional statistics were carried out using the circular statistics toolbox from [20]. Additionally, we display in Figure 3 the scatter plots for the M6 buoy.

As can be observed, the quality of this data in the offshore is good with a very low bias and RMSE values for the wind speed of less than 2m/s. The correlation coefficients are mostly above 0.9 for both speed and direction. However, the directional statistics do show some negative bias in the wind direction. As can be seen in Table I, the directional biases for M1, M2 and M4 (which are closer to the coast) are larger than for the M6 buoy, which is the farthest offshore. Overall, the OA performs slightly better than the EI dataset, which have spatial resolutions of $0.125\,°/0.125\,°$latitude/longitude for the OA atmospheric model and $0.75\,°/0.75\,°$latitude/longitude for the EI dataset respectively. Due to its better performance and higher resolution, the OA was chosen as U_{10} forcing for the LAMs. However, it should be noted that for the nearshore, topographical features of the coast will have a significant influence on the wind profile. The resolution of the ECMWF OA analysis is still too coarse to fully capture these local effects and hence, ideally the wind input forcing should be downscaled to a higher temporal and spatial resolution.

TABLE I
M BUOY OBSERVATIONS VERSUS ECMWF U_{10} WIND SPEED AND DIRECTION

M1 (62090): 2001-2007	(53.127°N, 11.200°W)				
Model (n=8052)	**X**	**Bias**	**RMSE**	**r**	**SI**
OA Speed (m/s)	8.68	-0.05	1.44	0.94	0.17
EI Speed (m/s)	-	-0.24	1.56	0.93	0.18
OA Dir (deg)	235.6	-3.82	14.59	0.95	0.12
EI Dir (deg)	-	-4.32	14.67	0.95	0.12
M3 (62092): 2003-2011	(51.217°N, 10.551°W)				
Model (n=11337)	**X**	**Bias**	**RMSE**	**r**	**SI**
OA Speed (m/s)	8.55	0.07	1.40	0.93	0.16
EI Speed (m/s)	-	0.12	1.64	0.90	0.19
OA Dir (deg)	245.9	-4.38	13.81	0.95	0.12
EI Dir (deg)	-	-5.55	15.93	0.94	0.14
M4 (62093): 2007-2011	(54.998°N, 09.992°W)				
Model (n=4842)	**X**	**Bias**	**RMSE**	**r**	**SI**
OA Speed (m/s)	9.18	0.19	1.41	0.94	0.15
EI Speed (m/s)	-	0.30	1.75	0.92	0.19
OA Dir (deg)	233.9	-3.43	14.58	0.94	0.12
EI Dir (deg)	-	-4.31	16.66	0.91	0.13
M6 (62095): 2006-2011	(53.074°N, 15.881°W)				
Model (n=6170)	**X**	**Bias**	**RMSE**	**r**	**SI**
OA Speed (m/s)	9.41	-0.45	1.43	0.97	0.15
EI Speed (m/s)	-	-0.20	1.51	0.95	0.16
OA Dir (deg)	244.5	-1.20	12.77	0.96	0.11
EI Dir (deg)	-	-2.0	13.67	0.95	0.12

III. LOCAL AREA MODELS SET-UP

In addition to the boundary input and the wind forcing, the quality and the resolution of the bathymetric data has a great influence on the accuracy of nearshore wave models. At the same time, archived sea-bed surveys present significant uncertainties which the hydrographic community has only recently started to address in a systematic fashion [21]. These uncertainties could be caused by either the survey methodology (geo-positioning errors for instance), interpolation techniques employed in the reconstruction of the continuous surface from the scattered survey data or actual changes in the sea-bed topography. Intensive campaigns, for instance the Integrated Mapping For the Sustainable Development of Ireland's Marine Resource (INFOMAR) which is a successor to the Irish National Seabed Survey (INSS) (as described in [22]), are in progress to map the nearshore areas with modern survey techniques such as light detection and ranging (LIDAR) or multi-beam echo-sounder (MBES) [23]. The coverage for the Irish Coast in the nearshore is still limited however, and it will probably take many years for a contiguous mapping to become available. In the mean time, ocean modelers have to rely on building digital elevation models (DEMs) that combine sets of data with varying degrees of accuracy and resolution ranging from historical chart derived data to modern surveys of high precision such as MBES and LIDAR. In this context, it is paramount to be able to ascertain the level of confidence one could have in the resulting DEM. Uncertainties in the bathymetry will undoubtably induce uncertainties in the hydrodynamical models and if not accounted for, could lead to erroneous interpretations of the modeling results, as [21] points out. Constructing DEMs with uncertainty estimates has been undertaken only in recent years - see for instance [24].

That being said, while recognizing the importance of the issues mentioned above, we do not pursue this particular aspect in our study and take a markedly simplified approach. The bathymetric grids for the two local area models have been obtained by merging lower resolution/higher uncertainty vector data derived from the United Kingdom Hydrological Office (UKHO) admiralty charts with high resolution/high precision

MBES INFOMAR survey data. The overlap areas between the two sets has been used to adjust the lower resolution set so as to avoid artificial ridges at the boundaries of the overlap. Such ridges are likely to induce spurious refraction effects and numerical instabilities in the hydrodynamical model. We outline the procedure below.

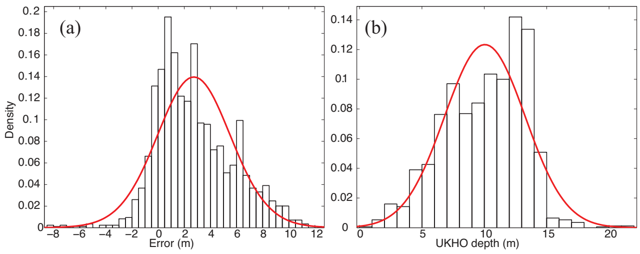

Fig. 4. (a) Histogram of the error on the overlap area between the MBES INFOMAR and UKHO datasets for the Achill region, depth bin 15-20m. (b) Histogram of the UKHO depths corresponding to the MBES INFOMAR depth bin 15-20m.

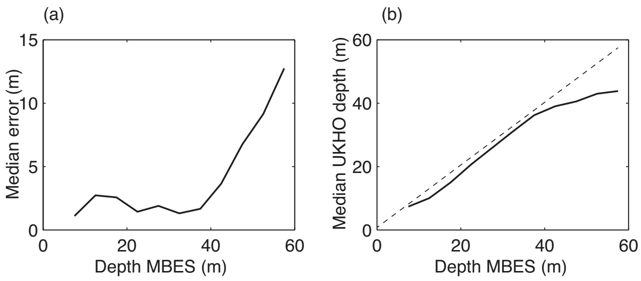

Fig. 5. Error analysis for the overlap area between the MBES INFOMAR and UKHO datasets for the Achill region. (a) Medians of the differences MBES-UKHO versus MBES depth bins centers. (b) Medians of the UKHO depths (on the MBES depth bins) versus MBES depth bins centers.

- First, the vector data from the two sources has been converted from Lowest Astronomical Tide surface to the Mean Sea Level by using the VORF software [25] obtained from the GSI.
- Next, the two sets (both consisting of scattered data of varying spatial resolution) have been gridded on a regular grid with a 2 arc-second resolution (or about 50-60m) by using a nearest-neighbor interpolation technique with a smoothing kernel to minimize aliasing error (in particular for the MBES INFOMAR data set which has a spatial resolution of approximately 5m). The error between the two sets can then be evaluated on the overlap area – see Figure 6, panel (a) for the Achill LAM case. Notice that in this case the mismatch between the two sets worsens with increasing depth, exceeding 10m at the western side of the overlap area. Also, we remark that the chart derived data consistently underestimates the depth. This systematic trend has been observed before in charted data and is commonly referred to as ”shoaling bias” [21], [26].
- The MBES gridded bathymetry has then been divided into depth bins (ranging from the minimum to the maximum depth on the patch - approx. 5m to 60m for the Achill LAM case). The difference between the two bathymetric sets has been estimated for all sets of points pertaining to each of the depth bins.
- For each MBES depth bin two histograms were constructed and then fitted with probability distribution functions (PDF):
  1) the histogram of errors;
  2) the histogram of chart derived data depths on the set of points pertaining to the MBES depth bin.

  In Figure 4 we depict these histograms for the Achill LAM case, depth bin 15 to 20m.
- The medians of the error PDF and the depth PDF were then derived for each MBES depth bin. In Figure 5 we depict these medians for the Achill LAM case, where depth bins of 5m where considered.
- Finally, a depth correction function for the chart derived data (correction as a function of depth contour) was constructed via interpolation from the two vectors of medians.

Through this procedure, the error is reduced considerably on the overlap region, as it can be seen in Figure 6, panel (b), and in particular at the boundaries – see Figure 7. We stress however that the underlying assumptions of this procedure are quite restrictive: the errors in the chart derived data are assumed to be correlated with depth, and homogeneous over the entire area of the chart derived data.

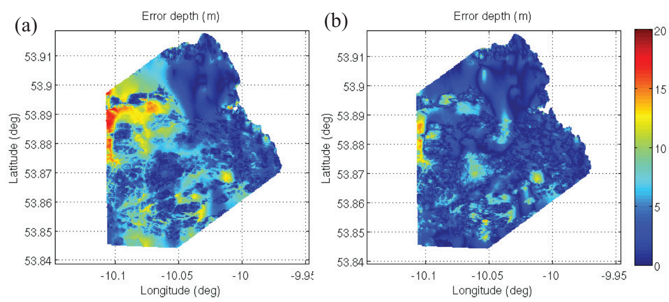

Fig. 6. (a) Absolute value of the error on the overlap area between the MBES INFOMAR and UKHO datasets for the Achill region. (b) Error after the median-based correction has been applied to the UKHO dataset.

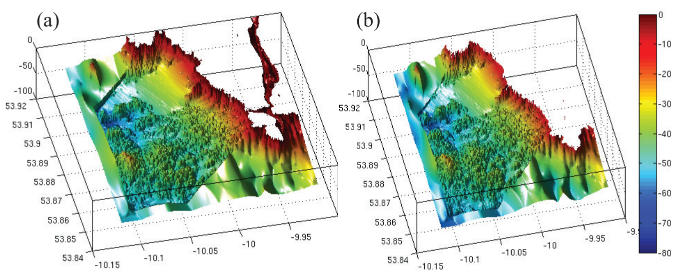

Fig. 7. Merged bathymetry for the Achill LAM. (a) No correction applied to the UKHO dataset. (b) The median-based correction applied to the UKHO dataset.

The final bathymetric grids are depicted in Figure 8. Each covers an area of approx. 1,000km^2. The offshore/western boundary points with depths over 50m are set as input boundary points. The coastline is taken on the 5m isobath. The computational grids are unstructured triangular meshes, with the highest resolution near coast (of approximately 50-100m).

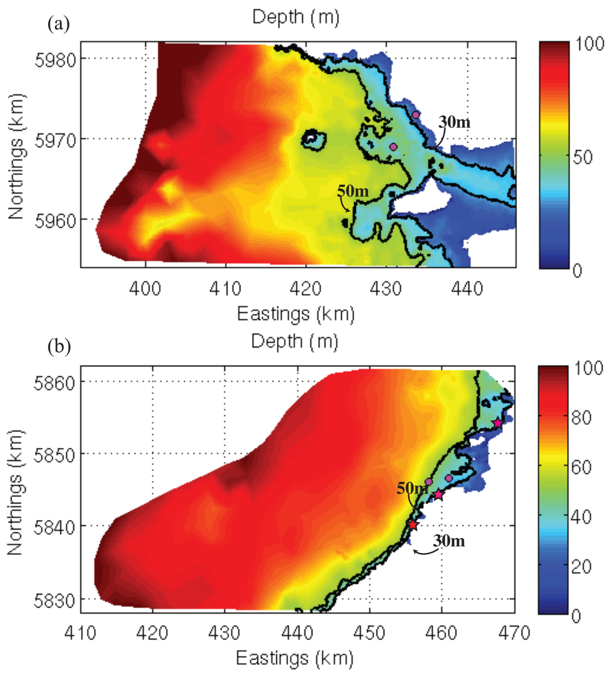

Fig. 8. (a) Achill and (b) Killard bathymetric grids. The horizontal coordinates are given in a Universal Transverse Mercator projection (29V). The 30m and 50m isobaths are depicted in each panel. Wave buoys used for validations are marked with circles. The red stars in panel (b) correspond to the points A, B, C in Figure 9 (from South to North).

IV. Results and Discussion

A. Validation and wave climate studies

An extensive validation study has been carried in [17] with directional buoy data obtained from the ESB. The ESB has deployed two Waverider directional buoys in the framework of the WestWave project: (1) one for the Achill area at 43m depth – see Figure 8(a); (2) one for the Killard area, with two deployment sites: at 51m and 36m depth respectively – see Figure 8(b). 10 months of data were available for the Achill Waverider, whereas only 3 months for each of the deployment sites at the Killard Point. Overall, excellent agreement between model and wave buoy data has been found for significant wave height, period and direction with biases in the significant wave height as low as 0.002m for the Achill 43m site and correlation coefficients for wave height and period exceeding 0.9.

A 10 year hindcast was carried out for the Killard LAM shown in Figure 8(a) – see [17] for details. There, we presented an analysis of the wave climate and energy resource, looking in particular at the variability across transects perpendicular to the coast and hence the correlation between the water depth and the wave energy resource. In addition, with the deployment of the first full scale WEC prototypes in the last few years, it has become apparent that the issue of accessibility for maintenance is at least as important as the presence of high levels of exploitable wave energy [27]. Our study revealed a greater level of accessibility at the Achill and Killard sites when compared to the AMETS test site in the Belmullet peninsula (Co. Mayo), while maintaining a considerable level of energy resource [17] .

In this study, we focused on the variability of the resource along the coastline and the effects induced by the coastline complexity. To this end in Figure 9 we display the year averages (for 2011-2012) of the significant wave height and wave power per metre of wavecrest on the 30m contour for the Killard LAM, Figure 8(b). Additionally, we display the bottom slope variation along this isobath. The slope was computed by taking the gradient of the bottom elevation, after conversion of the horizontal coordinates to eastings and northings (UTM, zone 29V). As it can be seen, there is a clear variability in the energy resource along this isobath.

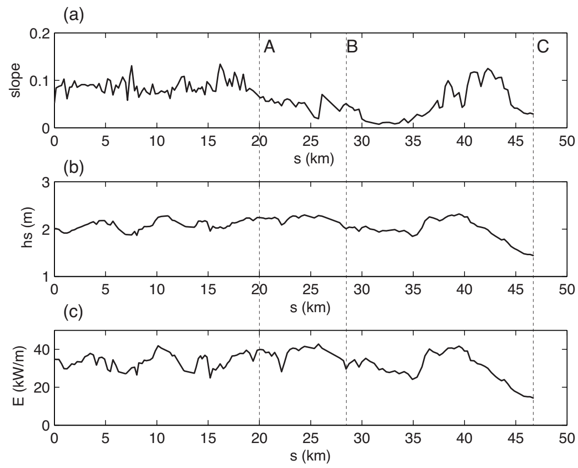

Fig. 9. Variation of (a) bottom slope, (b) significant wave height averaged over the year 2011-2012 and (c) omnidirectional wave power per metre of wave-crest averaged over the year 2011-2012, for the 30m isobath depicted in Figure 8, panel (b). The points A, B, C along the contour (marked with dashed line) correspond to the points marked with stars in Figure 8, panel (b) (from South to North).

B. Effects of reflection on the wave model performance

The improved DEM for the Achill LAM (constructed for this study as described in §II) improved considerably the performance of the model at shallower depths, as is evident in Figure 13(a) where a comparison for the significant wave height can be seen between the wave model and data from an Acoustic Doppler Current Profiler (ADCP) deployed by the ESB at the 21m depth contour. In the remainder of the section we focus on the effects of reflection parametrization on the wave model prediction using the improved DEMs and data from two Waverider buoy locations (at 43m in Achill and 36m in Killard) and the ADCP (at 21m in Achill).

Traditionally, the coastline in phase averaged spectral models is treated in a similar fashion to any open boundary, namely the energy incident on a boundary segment is propagated out of the computational domain. At the same time, field measurements have pointed out that the energy flux incident upon the coastline (not dissipated by bottom friction, wave breaking in the surf zone, etc.) can be reflected back towards the offshore [28]. It has been shown that in certain circumstances (and particularly for complex shorelines with steep gradients) it can enhance considerably the wave heights [29].

The field experiments of [28] confirmed Miche's [30] empirical formula:

$$R^2 \approx \frac{16g^2}{(2\pi)^5}\frac{\tan^5\beta}{H_\infty^2 f^4},$$

where R^2 is the ratio between the incident and reflected energy, β is the beach-slope/shore-face angle, H_∞ and f are the height and frequency respectively of the incident waves. As it can be seen from the above formula, the longer/lower frequency waves (swells) are reflected to a greater extent than the wind sea waves, the reflection is inversely proportional with wave height, and increases with increased seabed slope. The same field experiments in [28] indicate that the reflection is predominately specular (i.e. the reflected and incident waves are symmetric with respect to the local normal to the shoreline). Thus, reflection is expected to affect more the directionality of the wave field rather than the wave height.

In the context of nearshore wave models, the issue of reflection is interesting for two reasons. Firstly, directionality is important for marine operations in the nearshore and in particular for renewable energy installation and site selection [5], [17], [31]. Furthermore, near steep coastlines, reflection is going to affect directionality even in normal operating conditions for WECs, that is for moderate wave heights. Secondly, accounting for reflection considerably increases the correlation between the observed ocean-generated seismic noise and wave model simulated second order pressure spectrum, as [8] have demonstrated. Indeed, reflection affects long waves predominantly and interactions between opposing long waves (in the coastal region incident and reflected) enhance the second order pressure spectrum at low frequencies [8], [32]. This in turn is a source of seismic noise [8], [33].

Recently, reflection has been implemented in the WAVEWATCH III wave model – see [8], [33] for a detailed description of the implementation. In short, this process is modeled as a source term in the right hand side of the wave balance equation [34], specified at the nodes of the boundary which correspond to the coastline (in the case of unstructured triangular grids, as the ones that we are using in our LAMs). It is possible to specify a reflection coefficient R^2 which varies along the coastline, which in turn would afford a realistic representation of complicated shores such as those found in the west of Ireland. The essential ingredient in determining the reflectivity of a coast is the seabed slope at the water-land line. However, modern sea-bed surveys go only up to maximum of 5m depth. Typically, the slope on the shoreline is larger than the bathymetry gradient in the adjacent shallow areas [8] but there is no systematic correlation between the two. This could be seen in fact for the both the Achill and Killard areas (Figures 11 and 12) by contrasting the sea-bed slope evaluated from the bathymetric grid to aerial pictures of the coast (obtained and reproduced from the 2003 Coast of Ireland Oblique Imagery Survey with permission from the Office of Public Works OPW, Ireland).

In order to accurately capture the slope of the shoreline, one needs LIDAR datasets that straddle the littoral from the onshore to the shallow depth range. Such data is sparse for Ireland, at least on the west coast. According to [35] there are two agencies that currently collect LIDAR data here that meet the above criteria. Firstly, LIDAR datasets that extend to the 10m inland contour are available from the GSI/Marine Institute for a number of bays on the west coast. The OPW has also undertaken such LIDAR surveys which cover most of the east coast but only three bays on the west coast (as of 2011): Sligo, Galway and Tralee bays [35].

In the absence of LIDAR datasets in the areas of interest (which would enable an accurate estimate of the position of the shore and of the shore-face slope) we have chosen the shoreline boundary to be at the 5m depth isobar – as in [8]. This depth is also close to the boundary of the surveyed INFOMAR data available. Furthermore, one could argue that for steep bathymetric slopes, very high spatial resolution would be needed in this depth range which would also limit the overall time step due to the CFL condition, and hence be impractical to implement. Furthermore, we have found that the Global Self-consistent Hierarchical High-resolution Shoreline (GSHHS) database [36], which is often used to define the shoreline boundary in wave models, does not have sufficient accuracy for the scale of shoreline detail we aim to resolve. Indeed, by comparing the GSHHS (the full resolution version at 40m) to LANDSAT satellite imagery for Achill and Killard region, we found that the GSHHS crosses into the INFOMAR data set at depths greater than 20m in places. This can be seen in Figure 10 where the GSHHS shoreline is displayed overlaid on a LANDSAT image of the area and the INFOMAR MBES survey for the Achill area. In the absence of high resolution bathymetry on the shoreline, the best alternative to the GSHHS for high-resolution applications would be the vector high-water mark available from the Ordnance Survey of Ireland.

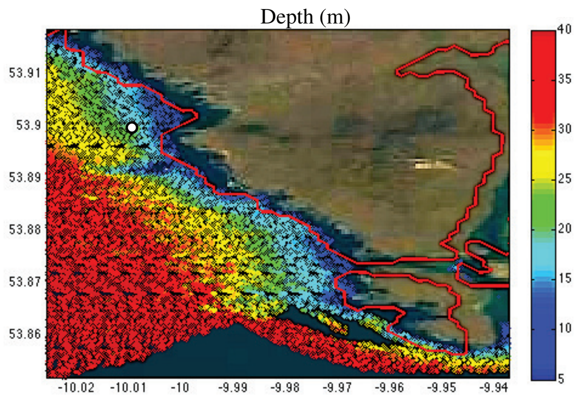

Fig. 10. GSHHS overlaid over a georeferenced LANDSAT image (retrieved from [37] using Matlab Mapping Toolbox) and INFOMAR MBES dataset (points with depths of over 5m where depicted) for the Achill Island area. The ADCP position is marked with a white circle.

Fig. 11. Upper panel: sea bed slope for the Achill local area model. Insets: aerial photographs of the coast for three location along the Achill coast. Images obtained and reproduced from the 2003 Coast of Ireland Oblique Imagery Survey with permission from the Office of Public Works (OPW), Ireland.

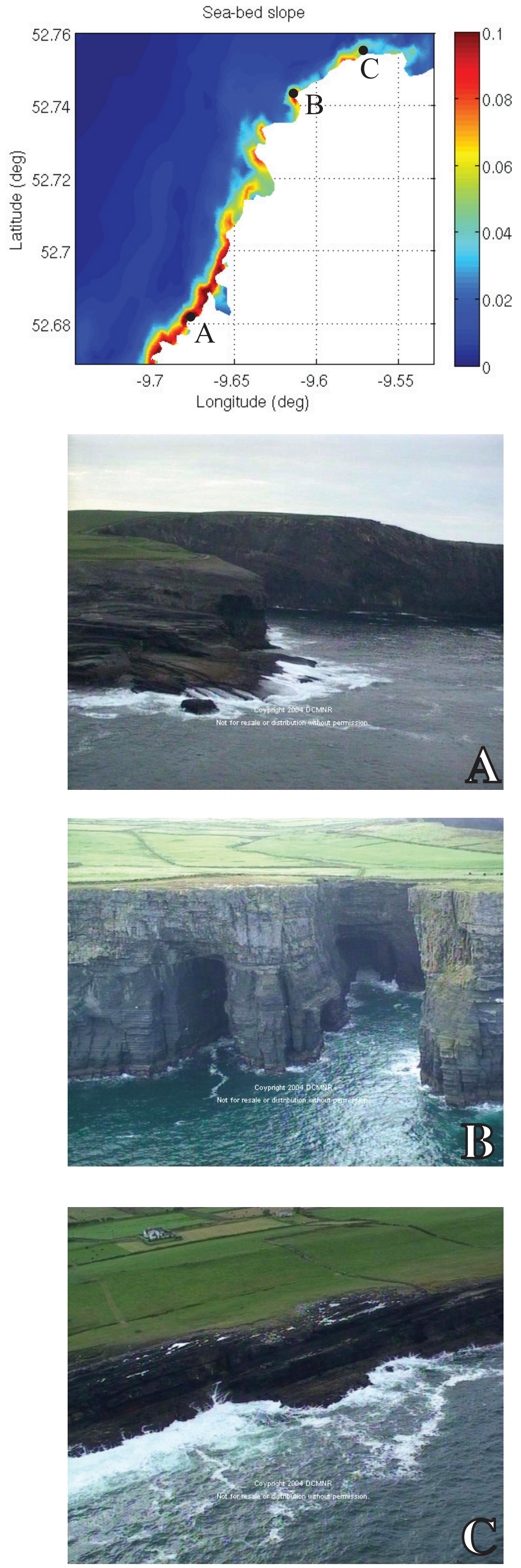

Fig. 12. Upper panel: sea bed slope for the Killard local area model. Insets: aerial photographs of the coast for three location along the Killard coast. Images obtained and reproduced from the 2003 Coast of Ireland Oblique Imagery Survey with permission from the Office of Public Works (OPW), Ireland.

As a first attempt to quantify the effects of coastal reflection on the performance of the wave model, we chose a series of uniform reflection coefficients R^2 along the coast ranging between a moderate 7% to a relatively strong 25%. As it can be seen in Figures 13 and 14, there is very little change in the significant wave height at both sites in the Achill LAM.

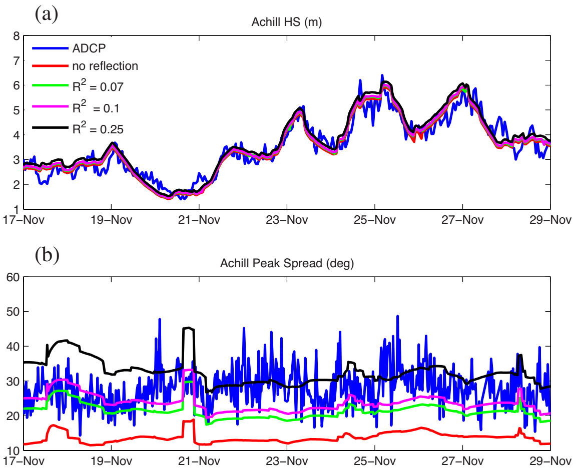

Fig. 13. (a) Significant wave height and (b) peak directional spread at the ADCP Achill (21m depth).

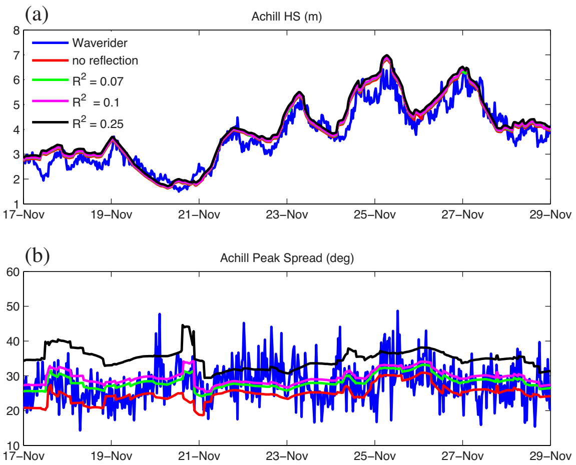

Fig. 14. (a) Significant wave height and (b) peak directional spread at the Waverider Achill (43m depth).

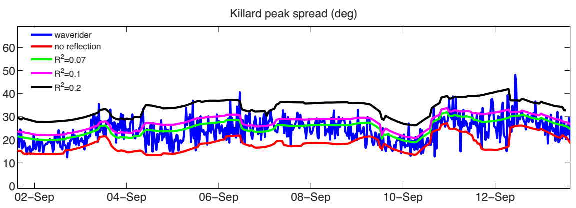

Fig. 15. Peak directional spread at the Waverider Killard (36m depth).

Nonetheless, the model without reflection under-predicts the peak directional spread. At the same time, we note that as remarked in [8] some buoys can have directional spread biases of the order of 5°. However, the disagreement between model and measurements without reflection are all of the order of 10°. Another caveat consists of our use of the peak directional spread as a diagnostic for quantifying the effects of reflection parametrization on directionality. The mean directional spread as defined in [38] and used in [8] would have been preferable but the peak spread was the only directional spread parameter available for both the WaveRider buoys and the ADCP.

Considering a 10% reflection coefficient improves considerably the directional spread, in particular at higher-depth Waverider buoys - as Figures 14(b) and 15 show. Indeed locations which are further away from the coastline "feel" the influence of reflected waves from a larger portion of the coast and, in a sense, the local topological intricacies of the shoreline are averaged out. In contrast, the sites closer to the coastline are expected to be more sensitive to the local shoreface slope. This could be the reason why at the ADCP site a higher reflection coefficient is needed (higher than 10%) in order to capture the directional spread – see Figure 13(b). Additionally, note that at the ADCP site, the bias in the peak directional spread of the model without any reflection, is substantially larger than at the deeper sites. Indeed, at shallower depths, refraction is expected to reduce the directional spread of the incident waves. As it can be seen in Figure 13(b) the measured directional spread is as high as at the Waverider buoy location. This could be in fact attributed to reflection at the coastline, which in this region is quite steep (as evidenced in panel (A) of Figure 11).

V. Conclusions

The ECMWF OA wind data off the West Coast of Ireland was assessed by comparison to data from the Irish Marine Buoy Network. The results indicate the high quality of this data in the offshore; nonetheless a downscaling to higher temporal and spatial resolution might be necessary near the coast where topographic features will cause a distortion in the wind-flow at smaller scales.

DEMs were built for the Achill and Killard areas. Our study shows that care needs to be taken with the construction of DEMs, in particular for nearshore applications on the Irish West Coast. High resolution bathymetry data still has a lot of lacunae here and it will likely take several years before complete coverage is achieved. The historical charted data for this region should be used with caution as a "shoaling bias" is present. This bias can be substantial as a percentage of the water depth (see Figure 5) and hence impact the accuracy of the wave model in the nearshore. The improved Achill DEM lead to a marked improvement of model results at the ADCP site (21m depth).

Finally, by comparison to buoy data, we bring some preliminary indications that reflection plays an important role in the wave climate on the West Coast of Ireland, where steep bathymetric slopes and complex rocky shorelines are common-place. Although accounting for reflection does not affect substantially the model predicted significant wave height, the predictions for the directional spread were considerably improved.

Acknowledgments

This study was funded by Science Foundation Ireland (SFI) under the research project "High-end computational modelling for wave energy systems". The ESB, Met Éireann and the Marine Institute provided the buoy data for validation. The INFOMAR bathymetric datasets were provided by the Geological Survey Ireland (GSI) and the Marine Institute. The VORF software for tidal datum conversions was obtained from the GSI. The authors would like to thank K. Verbruggen, S. Cullen and C. McKeon in the GSI for their help. The Office of Public Works (OPW) Ireland has given us access to their database of aerial photographs of the Irish coast (from the 2003 Coast of Ireland Oblique Imagery Survey), with particular thanks to J. Casey and B. Tyther at the OPW. We also thank M. Osborne (OCEANWISE) for his help with the UKHO bathymetry and for pointing out the "shoaling bias" of charted data. The authors thank Dr. C. Sweeney and Prof. P. Lynch (UCD School of Mathematical Sciences) for very helpful discussions and Dr. F. Ardhuin (Ifremer) for his advice regarding the WAVEWATCH code. We would also like to thank M. Béchereau for her help with the INFOMAR bathymetric datasets. Finally, the numerical simulations were performed on the Stokes cluster at the Irish Centre for High-end Computing (ICHEC).

References

[1] "Accessible wave energy resource atlas of Ireland." ESB International, Tech. Rep. Report 4D404A-R2 for the Marine Institute and Sustainable Energy Ireland, 2005.

[2] M. Curé, "A fifteen year model based wave climatology of Belmullet, Ireland," A report prepared on behalf of the Sustainable Energy Authority of Ireland (SEAI)., Tech. Rep., 2011.

[3] A. Rute Bento, P. Marinho, R. Campos, and C. Guedes Soares, "Modelling wave energy resources in the Irish West Coast," in *Proceedings of the 30th International Conference on Ocean, Offshore and Artic Enginnering OMAE*, Rotherdam, Netherlands, 2012.

[4] B. Cahil and A. Lewis, "Long term wave energy resource characterization of the Atlantic Marine Energy Test Site." in *Proceedings of the 9th European Wave and Tidal Energy Conference*, Southampton, U.K., 2011.

[5] M. Folley and T. Whitthaker, "Analysis of the nearshore wave energy resource," *Renewable Energy*, vol. 34, pp. 1709–1715, 2009.

[6] H. Tolman, "User manual and system documentation of Wavewatch III version 3.14," NOOA/NWS/NCEP/MMAB, Tech. Rep. 276, 2009.

[7] ESB WestWave project. [Online]. Available: http://www.westwave.ie/

[8] F. Ardhuin and A. Roland, "Coastal wave reflection, directional spread and semi-acoustic noise source." *Journal of Geophysical Reserch*, vol. 117, 2012.

[9] F. Ardhuin, E. Rogers, A. Babanin, J.-F. Filipot, R. Magne, A. Roland, A. van der Westhuysen, P. Queffeulou, J.-M. Lefevre, L. Aouf, and F. Collard, "Semi-empirical dissipation source functions for wind-wave models: part I, definition, calibration and validation," *Journal of Physical Oceanography*, vol. 40, no. 9, pp. 1917–1941, 2010.

[10] H. Gunther, P. Lionello, P. Janssen, A. Bertotti, C. Bruning, J. Carretero, L. Cavaleri, L. Guillaume, B. Hansen, S. Hasselmann, K. Hasselmann, M. de las Heras, V. Hollingsworth, M. Holt, J. Lefevre, and R. Portz, "Implementation of a third generation ocean wave model at the European Centre for Medium Range Weather Forecasts." ECMWF, Reading, Final report for EC Contract SC1-0013-C(GDF), 1992.

[11] P. A. E. M. Janssen, "Progress in ocean wave forecasting," *Journal of Computational Physics*, no. 227, pp. 3752–3594, 2008.

[12] P. Bechtold, M. Köchler, T. Jung, F. Doblas-Reyes, M. Leutbecher, M. J. Rodwell, F. Vitart, and G. Balsamo, "Advances in simulating atmospheric variability with the ECWMF model: from synoptic to decadal time-scales." *Q.J.R. Meterol. Soc.*, vol. 134, pp. 1337–1351, 2008.

[13] Marine Institute buoy network. [Online]. Available: http://www.marine.ie/home/publicationsdata/data/buoys/

[14] A. Persson, "User guide to ECMWF forecast products," European Centre for Medium-Range Weather Forecasts (ECMWF), Shinfield Park, Reading, RG2 9AX, UK, Tech. Rep., October 2011.

[15] H. Bidlot, J-R, "Intercomparison of the performance of operational ocean wave forecasting systems with buoy data," *Weather and forecasting*, vol. 17, pp. 287–310, 2002.

[16] ——, "Verification of operational global and regional wave forecasting systems against measurements from moored buoys," World Meteorological Organization, JCOMM 30, 2002.

[17] S. Gallagher, R. Tiron, and F. Dias, "A detailed investigation of the nearshore wave climate and the nearshore wave energy resource on the west coast of Ireland," in *Proceedings of the ASME 2013 32nd International Conference on Ocean, Offshore and Arctic Engineering OMAE*, Nantes, France, 2013.

[18] NOAA National Data Buoy Center. [Online]. Available: http://www.ndbc.noaa.gov/station_page.php?station=62095&unit=M

[19] R. B. Stull, *An introduction to boundary layer meteorology*. Kluwer Academic Press, 1988.

[20] P. Berens, "CircStat: a MATLAB toolbox for circular statistics." *Journal of Statistical Software*, vol. 31, no. 10, 2009.

[21] B. Calder, "On the uncertainty of archive hydrographic data sets." *IEEE Journal of Oceanic Engineering*, vol. 31, no. 2, pp. 249–265, 2006.

[22] B. Dorschel, A. Wheeler, X. Monteys, and K. Verbruggen, *Atlas of the Deep-Water seabed: Ireland*. Springer, 2011.

[23] *Integrated Mapping for The Sustainable Development of Ireland's Marine Resource (INFOMAR): A Successor to the Irish National Seabed Survey. Proposal & strategy*, Dublin, Ireland, 2006.

[24] M. Poti, B. Kinlan, and C. Menza, *A biogeographic assessment of sea birds, deep sea corals and ocean habitats of the New York bight: science to support offshore spatial planning.* NOAA National Center for Coastal Ocean Science, 2012, ch. 2.

[25] R. Adams, I. Jonathan, M. Ziebart, J. Turner, and J. Oliveira, "Joining up land and sea – the UKHO/UCL vertical offshore reference frame." *Hydro International*, vol. 10, no. 10, 2006.

[26] Comparison of surveyed and charted bathymetry. [Online]. Available: http://www.seazone.com/uploads/refzone-Comparison%20of%20Surveyed%20and%20Charted%20Bathymetry.pdf

[27] M. O'Connor, T. Lewis, and G. Dalton, "Weather window analysis of Irish west coast wave data with relevance to operations & maintenance of marine renewables," *Renewable energy*, no. 52, pp. 57–66, 2013.

[28] S. Elgar, H. Herbes, and R. Guza, "Reflection of ocean surface gravity waves from a natural beach," *Journal of Physical Oceanography*, vol. 24, no. 7, pp. 1503–1511, 1994.

[29] W. O'Reilly, R. Guza, and R. Seymour, "Wave prediction in the Santa Barbara channel, final techical report." http://www.coastalresearchcenter.ucsb.edu/cmi/files/2001-055.pdf, 1999.

[30] M. Miche, "Le pouvoir réfléchissant des ouvrages maritimes exposés à l'action de la houle," *Ann. Points. Chaussées*, vol. 121, pp. 285–319, 1951.

[31] A. Babarit, A. Hals, M. Muliwan, A. Kuriawan, T. Moan, and J. Krokstad, "Numerical benchmarking study of a selection of wave energy converters." *Renewable Energy*, vol. 41, pp. 44 –63, 2012.

[32] K. Hasselmann, "A statistical analysis of the generation of microseisms," *Rev. Geophys.*, vol. 1, no. 2, 1963.

[33] F. Ardhuin, E. Stutzmann, M. Schimmel, and A. Mangeney, "Ocean wave sources of seismic noise," *Journal of Geophysical Reserch*, vol. 116, 2011.

[34] G. Komen, G. Cavaleri, M. Donelan, K. Hasselmann, S. Hasselmann, and P. Janssen, *Dynamics and modelling of ocean waves*. Cambridge University Press, 1998.

[35] S. Coveney and X. Monteys, "Integration potential of INFOMAR airborne LIDAR bathymetry with external onshore LIDAR data sets," *Journal of Coastal Research*, vol. 62, pp. 19–29, 2011.

[36] P. Wessel and W. Smith, "A global self-consistent, hierarchical, high-resolution shoreline database," *Journal of Geophysical Research*, vol. 101, no. B4, pp. 8741–8743, 1996.

[37] C. NASA/JPL-Caltech. Global mosaic of Landsat7. [Online]. Available: http://ows.geogrid.org/basemap

[38] A. Kuik, G. van Vledder, and L. Holthuijsen, "A method for the routine analysis of pitch-and-roll buoy wave data," *Journal of Physical Oceanography*, vol. 18, pp. 1020–1034, 1988.